A detection of orbital radial velocity variations of the primary component in the black hole binary A0620 - 00 (= V616 Monocerotis)

Journal Item

THE ASTROPHYSICAL JOURNAL, 359:L47–L50, 1990 August 20

A DETECTION OF ORBITAL RADIAL VELOCITY VARIATIONS OF THE PRIMARY COMPONENT IN THE BLACK HOLE BINARY A0620−00 (= V616 MONOCEROTIS)

CAROLE A. HASWELL
McDonald Observatory and Department of Astronomy, University of Texas at Austin

AND

ALLEN W. SHAFTER[1]
Department of Astronomy, San Diego State University
Received 1990 March 26; accepted 1990 May 24

ABSTRACT

Time-resolved spectroscopic observations of Hα emission from the accretion disk in A0620−00 (V616 Mon) are presented. The emission exhibits radial velocity variations at the orbital period; the phase of the variations is shifted by $\sim 180°$ from the radial velocity curve of the K star. It is argued that these velocity variations reflect the orbital motion of the compact object. A semiamplitude, $K_1 = 43 \pm 8$ km s^{-1}, is derived, which, in conjunction with McClintock and Remillard's value of $K_2 = 457 \pm 8$ km s^{-1}, yields a mass ratio, q $(= M_1/M_2) = 10.6 \pm 2.0$. Potential systematic errors in our velocity measurements which would lead to increased uncertainty in the mass ratio are discussed. Taken at face value, our determination of the mass ratio results in new lower limits on the masses of the component stars: $3.82 \pm 0.24\ M_\odot$ for the compact object, strengthening the case that it is a black hole; and $0.36 \pm 0.07\ M_\odot$ for the K star. If the K star has a mass appropriate for a Roche lobe–filling main-sequence star, then the mass of the black hole could be as high as $11\ M_\odot$.

Subject headings: black holes — stars: accretion — stars: individual (A0620−00) — stars: X-rays — X-rays: binaries

I. INTRODUCTION

In 1975 the X-ray transient A0620−00 (Nova Mon 1917, 1975) underwent its most recent eruption, becoming the brightest X-ray source in the sky (Elvis *et al.* 1975). During the next 18 months the optical counterpart, V616 Mon, faded some 6 mag from $B \sim 12$ at the peak of the outburst to $B \sim 18.5$ at quiescence. Spectroscopic observations in quiescence revealed broad, double-peaked Balmer emission lines superposed on a K-type stellar absorption spectrum (Oke 1977). As in the case of a cataclysmic variable, the broad emission was attributed to an accretion disk surrounding the compact object (the primary), while the absorption spectrum was identified with the K-type companion (the secondary).

Extensive observations during the 1980s established A0620−00 as arguably the best black hole candidate yet discovered. Photometry and spectroscopy by McClintock and Remillard (1986) established the orbital period ($P = 0^d.323014$) and revealed radial velocity variations of the K star with an amplitude of 457 ± 8 km s^{-1}. The corresponding mass function is $f(M) = 3.19 \pm 0.17\ M_\odot$, which exceeds the maximum allowed mass for a neutron star (Arnett and Bowers 1977). Recently, Johnston, Kulkarni, and Oke (1989) obtained spectroscopic observations that enabled them to confirm the mass function and to further constrain the mass of the black hole from models of the disk emission.

A0620−00 offers the best opportunity to measure the mass of a black hole directly. Unlike two of the other three leading candidate black hole binaries, Cyg X-1 (Gies and Bolton 1986) and LMC X-3 (Cowley *et al.* 1983), the compact object in A0620−00 appears to be encircled by a fully developed accretion disk. The other candidate, Cal 87, appears to be similar in structure to A0620−00 and is eclipsing; however, the mass-losing star is observed only during eclipse (Cowley *et al.* 1990). Consequently, the compact object's mass function is undetermined and the mass estimates for Cal 87 are currently based on indirect arguments.

Since the radial velocity semiamplitude of the K star in A0620−00 is known, the mass ratio of the system can be determined from a measurement of radial velocity variations of the disk emission. The mass ratio, coupled with a knowledge of the orbital inclination, yields the mass of the black hole directly. In principle, the orbital inclination of A0620−00 may be constrained from ellipsoidal variations of the K star, and that work is in progress (Haswell *et al.* 1990). In this *Letter*, we report the determination of the mass ratio of A0620−00 based on time-resolved spectroscopy of the Hα emission line.

II. OBSERVATIONS

Observations of A0620−00 were obtained using the Large Cassegrain Spectrograph at the Cassegrain focus of the McDonald Observatory's 2.7 m reflector. The spectra were recorded using a thinned TI CCD chip. Data were acquired on the nights of 1989 December 29, December 30; 1990 January 1, and January 2 U.T. We used a 2″ slit which matched the seeing and resulted in a spectral resolution of about 3 Å FWHM. The spectra cover the range 6245–6952 Å at a dispersion of 0.88 Å per pixel. We performed 30 minute integrations on the object, recording a neon lamp exposure after each object spectrum. The spectrograph was stable; the wavelength scale exhibited a steady drift of order 0.1 pixels hr^{-1}.

The reductions were carried out primarily using IRAF; however, an IDL routine was used for the optimal extraction of the one-dimensional spectra. Wavelength calibration was achieved by interpolating between the neon spectra taken

[1] Guest Observer, McDonald Observatory.

immediately before and after each object exposure. Since the wavelength changes were steady, we are confident that our interpolations are accurate and estimate internal errors of ± 5 km s^{-1}. We did not observe a radial velocity standard, so our wavelength scale may be subject to a zero-point offset of order 3 Å (the resolution element).

III. DISCUSSION

a) *The Line Profile*

The emission lines seen in the spectrum of A0620−00 are characteristic of emission from accretion disks in cataclysmic variables. In addition to the usual double-peaked structure, the emission reveals an s-wave disturbance at a phase close to that of the K star, presumably associated with the impact of the mass transfer stream with the disk (Johnston, Kulkarni, and Oke 1989). To examine the changes in the structure of the Hα profile with orbital phase, we co-added the spectra into 10 orbital phase bins. In our convention, phase 0.0 corresponds to superior conjunction of the compact object; this is 180° out of phase with the photometric ephemeris of McClintock and Remillard (1986). The co-added spectra are shown in Figure 1. The profiles are clearly double peaked, with a peak-to-peak separation of ~ 1200 km s^{-1}. The s-wave feature, while substantially weaker, has a phasing consistent with that seen by Johnston, Kulkarni, and Oke (1989). A narrow central peak is seen migrating from blue to red in the phase 0.8–0.1 spectra; this is predicted by models in which the hot spot is localized at the outer edge of the disk (Johnston, Kulkarni, and Oke 1989).

Our grand sum line profile is shown in Figure 2. This spectrum was obtained by normalizing the phase-resolved spectra so that the total flux in the line was the same for all phases, then adding them. The data are compared with a model profile

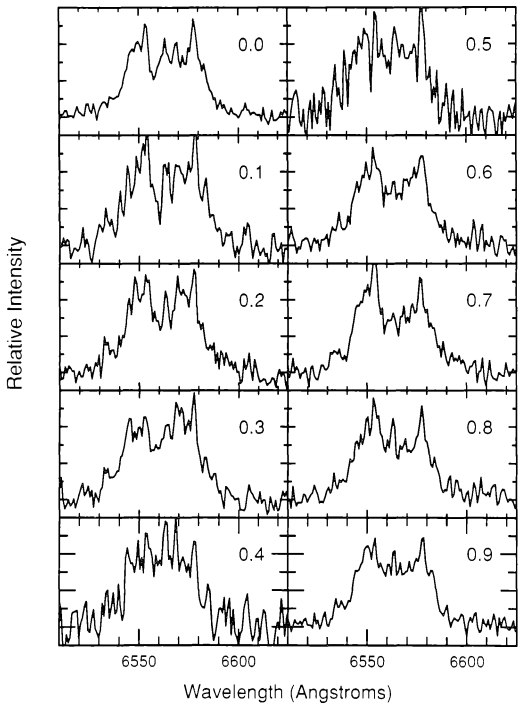

FIG. 1.—The phase-resolved spectra. The s-wave component can be seen as a third, central peak, migrating from blue to red at orbital phases 0.8, 0.9, 0.0, and 0.1.

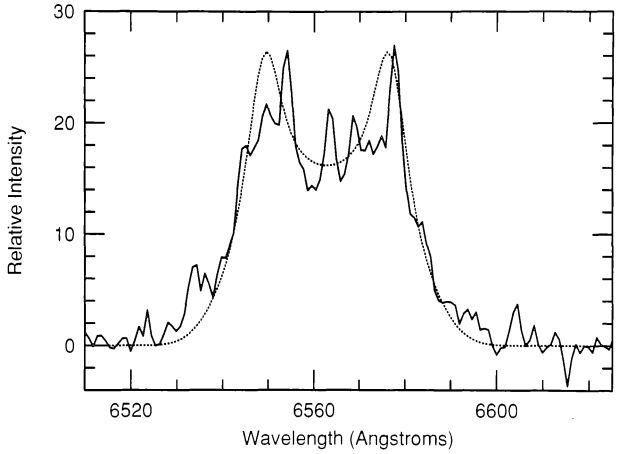

FIG. 2.—The grand sum line profile and, for comparison, a symmetrical model line profile (*dotted line*). The observed profile is asymmetric; the narrow peaks are displaced to the red, and there appears to be excess emission in the blue wing of the line. The parameters of the model profile are projected velocity at the outer edge of the disk = 600 km s^{-1}, ratio of outer to inner radii = 4.8, surface brightness distribution $\propto r^{-1}$, and local line-broadening = 0.12 × projected Keplerian velocity.

that was computed using the algorithm described in Shafter, Szkody, and Thorstensen (1986). Unlike the grand sum profile obtained by Johnston, Kulkarni, and Oke (1989), our profile is distinctly asymmetric; the narrow peaks are redshifted with respect to the broader profile, and there is a suggestion of an excess emission component in the blue wing of the line.

b) *Radial Velocities*

As is the case with cataclysmic variables, the s-wave complicates attempts to infer the motion of the central object. To assess the extent of the phase-dependent asymmetries in the line profile, radial velocities were extracted in the manner often employed for cataclysmic variable data. This method involves convolving the data with a template spectrum consisting of two narrow Gaussians, one in each wing of the emission line. The zero-point of the template's wavelength scale is adjusted until the value of the convolution is the same in both Gaussians. The midpoint between the two Gaussians then provides a measure of the wavelength of the line. By varying the separation of the Gaussians, different parts of the line profile are sampled, and the phase-dependent structure of the emission may be studied.

Initially we measured velocities for the 35 individual spectra using Gaussians with widths of 250 km s^{-1} (FWHM) and a separation of 900 km s^{-1}. The resulting velocities were then fitted to sinusoids of the form:

$$V(t) = \gamma - K_1 \sin\left(\frac{t - t_0}{P}\right),$$

where the orbital period, P, the time of superior conjunction of the compact object, t_0, and the systemic velocity, γ, were initially unconstrained. The best fit yielded the following orbital elements: $P = 0^d.3226 \pm 0^d.0018$; $K_1 = 44 \pm 8$ km s^{-1}; $t_0 = 2{,}447{,}893.853 \pm 0.011$; $\gamma = -25 \pm 5$ km s^{-1}. We are confident that the velocity variations result from the orbital motion of the compact object. The observed variations occur with a period consistent with the orbital period *and* with a phase that is shifted by $\sim 180°$ relative to that of the K star. The observed phasing rules out any possibility that the varia-

tions might be due solely to hot spot contamination, although, as we discuss below, the s-wave emission may spuriously *lower* the measured amplitude.

To refine the velocity amplitude, we measured the radial velocities for our 10 phase-resolved spectra. We again used 250 km s^{-1} FWHM Gaussians, whose separation was varied from 1400 km s^{-1} to 3000 km s^{-1}, in 200 km s^{-1} intervals. This procedure yielded a total of nine measurements for each phase. The nine sets of velocities were then fitted to circular orbits. The resulting orbital elements are plotted as a function of the Gaussian separation in Figure 3, forming a "diagnostic diagram." Descriptions of diagnostic diagrams and their interpretation are given in Shafter, Szkody, and Thorstensen (1986) and Shafter (1985).

The diagnostic diagram is useful for assessing the degree of contamination by nonaxisymmetric emission. Any phase-dependent asymmetry will cause the orbital elements to vary with Gaussian separation. It is usually desirable to extract orbital velocities using relatively large Gaussian separations. If the contamination is confined to the outer disk, as is usually assumed in the case of hot spot emission, the orbital elements should converge to their true values as the Gaussian separation is increased. Referring to the error bars in Figure 3, we see that beyond a Gaussian separation of $\sim$1800 km s^{-1}, the measurements begin to become increasingly affected by noise in the extreme line wings and continuum. The orbital elements determined using a Gaussian separation of 1800 km s^{-1} are as follows: $K = 43 \pm 8$ km s^{-1}, $\gamma = -28 \pm 6$ km s^{-1}, and $\Delta\phi = 59° \pm 11°$. The corresponding radial velocity curve is shown in Figure 4.

We cannot be certain that the K-velocity determined using a Gaussian separation of 1800 km s^{-1} accurately reflects the amplitude of the compact object's orbital motion. In particular, the observed phase shift of $\sim$60° (0.16 in orbital phase) is disconcerting. Only about half of this shift may be accounted for by the cumulative phase error which results from the use of McClintock and Remillard's (1986) orbital elements in phasing our spectra. The remaining phase shift is likely a result of

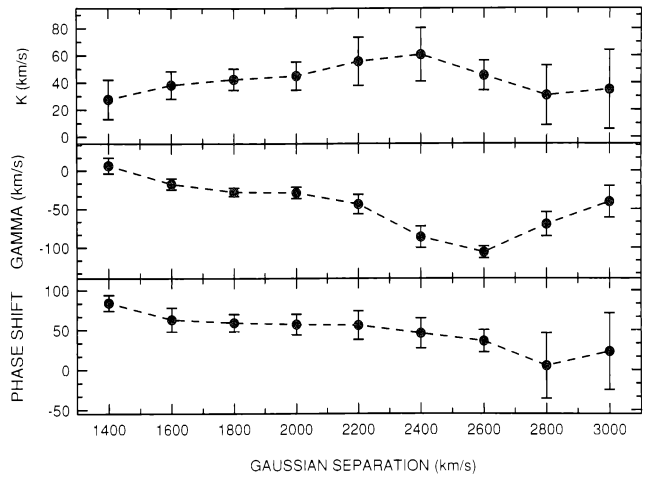

FIG. 3.—The diagnostic diagram for A0620−00. The derived orbital elements are plotted as a function of the Gaussian separation used in the velocity measurements. The best-fitting semiamplitude ($K_1 = 43 \pm 8$ km s^{-1}) occurs for a separation of 1800 km s^{-1}. The smallest error in the determination of the γ-velocity and phase shift also occur at a separation of 1800 km s^{-1}. (A phase shift of 0° is shifted by 180° with respect to the radial velocity curve of the K star.)

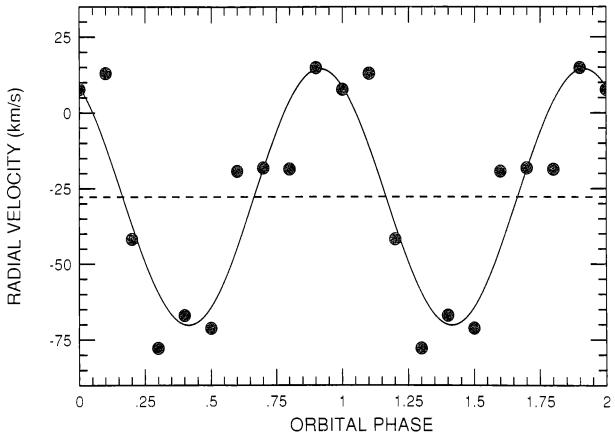

FIG. 4.—The radial velocity curve for the phase-binned spectra. The best-fitting sinusoid has an amplitude of 43 ± 8 km s^{-1}.

s-wave contamination of the disk line profile. Similar phase shifts are often noted in analyses of eclipsing cataclysmic variable radial velocity data (e.g., see Shafter, Hessman, and Zhang 1988; Stover 1981), and their nature is not fully understood. We have chosen to adopt orbital elements based on a separation of 1800 km s^{-1} for our analysis in part because the fit to a circular orbit is best at this separation. It is comforting to note that if we increase the separation to 2000 km s^{-1} (or to 2600 km s^{-1} for that matter) the K-velocity increases only slightly to 45 ± 10 km s^{-1}. We wish to stress that the error estimates quoted above reflect the formal errors of fits to sinusoids; the magnitudes of any systematic errors are potentially large and difficult to estimate.

There are at least three possible sources of contamination leading to systematic error in our amplitude determination: the s-wave emission, the secondary star, and the blueshifted component of the emission. Since the hot spot is apparently localized to the outer part of the disk, s-wave contamination should be minimal in the line wings. However, for small Gaussian separations, s-wave emission may spuriously reduce the radial velocity amplitude. The velocity amplitude of the K star, 457 km s^{-1}, is smaller than the velocity at the outer part of the disk, so it, too, is unlikely to contaminate the emission in the wings of the line. At small Gaussian separations, contaminating emission from the K star may reduce the measured radial velocity amplitude, while substantial Hα absorption from the K star could artificially increase the inferred amplitude. However, since we observe s-wave emission, any net absorption from the K star is apparently overwhelmed by emission from the hot spot. Thus, the combined effect of hot spot and K star contamination can only result in an underestimate of the radial velocity amplitude.

As the Gaussian separation increases from 1400 to 1600 km s^{-1}, the γ-velocity drops significantly; this is presumably due to the declining influence of the sharp, relatively red peaks in the line profile. The γ-velocity is essentially constant for Gaussian separations of 1800 and 2000 km s^{-1}, but as the separation is increased from 2000 to 2600 km s^{-1}, it drops sharply. This latter trend is likely caused by the excess emission component mentioned earlier, which is blueshifted by about 1300 km s^{-1} relative to the line center (see Fig. 2). The origin of this component is unknown, but it is possible that it arises in a wind from the accretion disk. We expect our adopted orbital elements, which are based on a separation of 1800 km s^{-1}, to be

the least contaminated by either the sharp low-velocity peaks or the blueshifted emission.

Finally, if we choose to be quite pessimistic, we could imagine one additional source of systematic error: non-Keplerian disk rotation. In this case nonaxisymmetric disk emission may cause spurious radial velocity variations to be introduced which could undermine our measurements. We assume this is not the case but cannot rule out the possibility.

c) *Mass Constraints*

Using the mass function, $f(M) = 3.19 \pm 0.17\ M_\odot$ (McClintock and Remillard 1986), loci of possible component masses have been computed for various orbital inclinations and plotted in Figure 5. Knowledge of both the inclination and the mass ratio together enables a unique solution for the component masses. The primary's mass is principally determined by the inclination, being only weakly dependent on the secondary star mass.

The orbital inclination is poorly constrained, though the lack of an X-ray eclipse (Elvis *et al.* 1975) means the inclination must be less than $\sim 85°$. We can constrain the mass of the compact object if, for the sake of discussion, we disregard possible systematic errors and take our results at face value. With $K_1 = 43 \pm 8$ km s^{-1} and $K_2 = 457 \pm 8$ km s^{-1} (McClintock and Remillard 1986), we find a mass ratio of $q = 10.6 \pm 2.0$. This raises the minimum allowed mass for the primary from 3.19 ± 0.17 to $3.82 \pm 0.24\ M_\odot$ for an inclination of 90°; the corresponding minimum mass for the secondary is $0.36 \pm 0.07\ M_\odot$.

Another constraint may be applied if we make the (likely) assumption that the mass of the secondary star must be less than or equal to that of a Roche lobe–filling main-sequence star. Patterson (1984) has derived an expression for the mass of Roche lobe–filling secondary stars in compact binaries. Using his calibration we find that $M_2 < 0.85\ M_\odot$ for an orbital period of $0^d.323$. Thus the component masses for the A0620−00 system most likely fall within the region in Figure 5 bounded by the heavy lines. In addition to the lower limit on M_1 set by the mass function and the upper limit on the inclination set by the absence of X-ray eclipses, a mass ratio of $q = 10.6 \pm 2.0$ in conjunction with $M_2 < 0.85\ M_\odot$ suggests an upper limit of $\sim 11\ M_\odot$ for M_1, and a lower limit to the inclination of $\sim 45°$. Finally, we note that if the secondary star has the mass of a K4–K7 dwarf (Oke 1977), the primary's mass is likely to lie in the range of 4–9 $M_\odot$. A precise determination of the mass of the primary will have to await a reliable estimate of the orbital inclination and further spectroscopy to improve the reliability of the mass ratio.

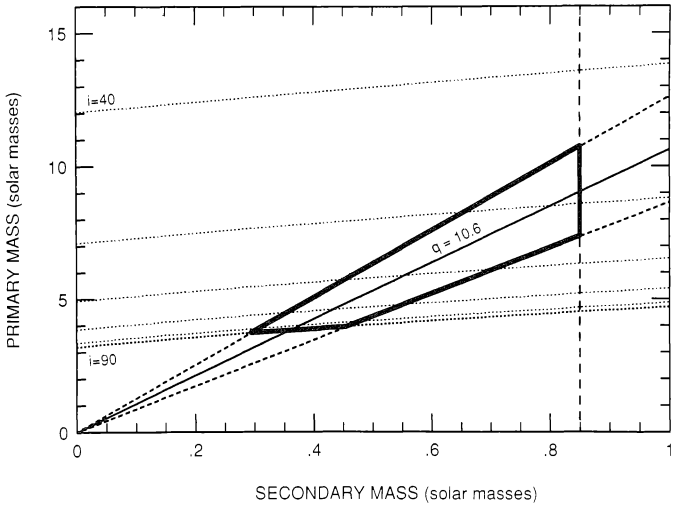

FIG. 5.—The allowed component masses for the A0620−00/V616 Mon system; K star mass along the abcissa, compact object mass along the ordinate. The dotted lines are loci of constant orbital inclination, ranging from $i = 40°$ to $i = 90°$ in 10° steps. The solid line represents our determination of the mass ratio, the associated dashed lines representing formal $\pm 1\ \sigma$ errors. The vertical broken line indicates the approximate mass of a Roche lobe–filling main-sequence star. The component masses are most likely to fall within the region bounded by the heavy lines.

d) *Conclusions*

We have detected the orbital motion of the compact object in A0620−00, obtaining a radial velocity amplitude $K_1 = 43 \pm 8$ km s^{-1}. This result may be subject to systematic errors of unknown magnitude, but in § III*b* we showed that our value of K_1 is more likely to be spuriously low than spuriously high. If K_1 is increased, the *minimum* mass of the compact object also increases; hence $3.82 \pm 0.24\ M_\odot$ is a reliable lower limit for the primary's mass and the case that A0620−00 is a black hole is strengthened. Further observations will enable K_1, and thus the mass ratio, to be determined to a higher accuracy.

This work was supported in part by NSF grant AST 87-04382. We thank C. Theodore Daub and E. L. Robinson for comments on the manuscript. C. A. H. gratefully acknowledges Zonta International for support from an Amelia Earhart fellowship, and the director of McDonald Observatory for the provision of travel funds. A. W. S. thanks McDonald Observatory for hospitality.

REFERENCES

Arnett, W. D., and Bowers, R. L. 1977, *Ap. J. Suppl.*, **33**, 415.
Cowley, A. P., Crampton, D., Hutchings, J. B., Remillard, R., and Penfold, J. E. 1983, *Ap. J.*, **272**, 118.
Cowley, A. P., Schmidtke, P. C., Crampton, D., and Hutchings, J. B. 1990, *Ap. J.*, **350**, 288.
Elvis, M., Page, C. G., Pounds, K. A., Ricketts, M. J., and Turner, M. J. L. 1975, *Nature*, **257**, 656.
Gies, D. R., and Bolton, C. T. 1986, *Ap. J.*, **304**, 371.
Haswell, C. A., Robinson, E. L., Horne, K. D., Stiening, R., and Abbott, T. M. C. 1990, in preparation.
Johnston, H. M., Kulkarni, S. R., and Oke, J. B. 1989, *Ap. J.*, **345**, 492.
McClintock, J. E., and Remillard, R. A. 1986, *Ap. J.*, **308**, 110.
Oke, J. B. 1977, *Ap. J.*, **217**, 181.
Patterson, J. 1984, *Ap. J. Suppl.*, **54**, 443.
Shafter, A. W. 1985, in *Cataclysmic Variables and Low Mass X-Ray Binaries*, ed. D. Q. Lamb and J. Patterson (Dordrecht: Reidel), p. 355.
Shafter, A. W., Hessman, F. V., and Zhang, E. H. 1988, *Ap. J.*, **327**, 248.
Shafter, A. W., Szkody, P., and Thorstensen, J. R. 1986, *Ap. J.*, **308**, 765.
Stover, R. J. 1981, *Ap. J.*, **249**, 673.

CAROLE A. HASWELL: Department of Astronomy, University of Texas, Austin, TX 78712

ALLEN W. SHAFTER: Department of Astronomy, San Diego State University, San Diego, CA 92182